Ultrasonic attenuation in magnetic fields for superconducting states with line nodes in Sr_2RuO_4

L. Tewordt and D. Fay
I. Institut für Theoretische Physik, Universität Hamburg, Jungiusstr. 9, D-20355 Hamburg, Germany
(Received 10 September 2001; published 14 February 2002)

We calculate the ultrasonic attenuation in magnetic fields for superconducting states with line nodes vertical or horizontal relative to the RuO_2 planes. This theory, which is valid for fields near H_{c2} and not too low temperatures, takes into account the effects of supercurrent flow and Andreev scattering by the Abrikosov vortex lattice. For rotating in-plane field $H(\Theta)$ the attenuation $\alpha(\Theta)$ exhibits variations of fourfold symmetry in the rotation angle Θ. In the case of vertical nodes, the transverse $T100$ sound mode yields the weakest (linear) H and T dependence of α, while the longitudinal $L100$ mode yields a stronger (quadratic) H and T dependence. This is in strong contrast to the case of horizontal line nodes where α is the same for the $T100$ and $L100$ modes (apart from a shift of $\pi/4$ in field direction) and is roughly a quadratic function of H and T. Thus we conclude that measurements of α in in-plane magnetic fields for different in-plane sound modes may be an important tool for probing the nodal structure of the gap in Sr_2RuO_4.

DOI: 10.1103/PhysRevB.65.104510 PACS number(s): 74.20.Rp, 74.25.Ld, 74.60.Ec, 74.70.Pq

I. INTRODUCTION

A number of experiments give evidence that the superconducting state in layered Sr_2RuO_4 (Ref. 1) consists of spin-triplet Cooper pairs with broken time-reversal symmetry. More recent experiments at low temperatures have established power-law T dependence of the specific heat (T^2),[2] the spin-lattice relaxation rate (T^3),[3] the electronic thermal conductivity,[4,5] the penetration depth,[6] and the ultrasonic attenuation.[7,8] These properties are most naturally explained in terms of a spin-triplet order parameter $\mathbf{d}(\mathbf{p})=\Delta\hat{\mathbf{z}}(p_x+ip_y)g(\mathbf{p})$ where the even-parity function $g(\mathbf{p})$ has vertical line nodes (e.g., $p_x^2-p_y^2$ or p_xp_y) or horizontal line nodes [e.g., $\cos(cp_z+a_0)$] on the cylindrical Fermi surface.[9–11] Since the measured anisotropy of the in-plane thermal conductivity $\kappa[\Theta]$ for rotating in-plane magnetic field[4] is smaller than the calculated anisotropy for vertical nodes,[11] and since the anisotropy of the interplane $\kappa[\Theta]$ is insignificant,[5] these authors have discarded vertical nodes and suggested instead horizontal nodes in the superconducting gap. Recently we have shown, however, that the amplitudes of $\kappa[\Theta]$ for vertical and horizontal line nodes are about the same.[12] The small size of the observed amplitude of $\kappa[\Theta]$ is due to the result that the amplitude of the variation of $\kappa[\Theta]$ decreases with increasing impurity scattering and temperature. The data for ultrasonic attenuation α in Sr_2RuO_4 measured for different sound directions $\hat{\mathbf{q}}$ and polarizations $\hat{\mathbf{e}}$ in the ab plane are found to be consistent with a vertical line node structure $p_x^2-p_y^2$ or a horizontal line of nodes in conjunction with significant gap modulation.[7]

Since the question as to the nodal structure of the superconducting gap in Sr_2RuO_4 is still unresolved, we suggest here measurements of the anisotropy of the ultrasound attenuation $\alpha(\Theta)$ for rotating in-plane magnetic fields. Indeed, ultrasonic attenuation is another powerful tool for probing the anisotropic gap structure because $\alpha(\Theta)$ is sensitive to the relative orientations of the sound direction and polarization, $\hat{\mathbf{q}}$ and $\hat{\mathbf{e}}$, the field $\mathbf{H}(\Theta)$, and the nodal directions of the gap. We shall show that $\alpha(\Theta)$ exhibits fourfold symmetric variations in rotation angle Θ of the magnetic field while the variations of $\kappa[\Theta]$ have twofold symmetry. It turns out that the field and temperature dependencies of α for vertical gap nodes are quite different for longitudinal and transverse sound modes while α for horizontal nodes is essentially the same for longitudinal and transverse sound modes. Thus observation of the field and temperature dependence of α for longitudinal and transverse sound modes should yield important information on the nodal structure of the gap in Sr_2RuO_4.

The ultrasonic attenuation α in the vortex state near H_{c2} for type-II s-wave superconductors has been calculated previously by Scharnberg[13] and by Klimesh and Pesch.[14] In Ref. 13 the Green's function G of Brandt, Pesch, and Tewordt (BPT) (Ref. 15) has been employed which was derived from the spatial Gorkov integral equation for $G(\mathbf{r},\mathbf{r}',\omega)$ with kernel proportional to the "potential"

$$V(\mathbf{r}_1,\mathbf{r}_2)=\Delta(\mathbf{r}_1)\Delta^*(\mathbf{r}_2)\exp\left(-2\imath e\int_1^2\mathbf{A}\cdot\mathbf{ds}\right),$$

where $\Delta(\mathbf{r})$ is the Abrikosov vortex-lattice order parameter and $\mathbf{A}$ is the vector potential of the magnetic field. This integral equation has been solved by expanding all functions in Fourier series $\mathbf{k}$ with respect to center-of-mass coordinates and in Fourier integrals $\mathbf{p}$ with respect to relative (difference) coordinates. In calculating physical quantities near H_{c2} it often suffices to consider only the $\mathbf{k}=0$ Fourier component $G(\mathbf{p},\omega)$. The corresponding anomalous Green's function F has been derived in the context of NMR theory by Pesch.[16] The effective self-energy part occurring in the denominators of these Green's functions is proportional to the spatial average of $|\Delta(\mathbf{r})|^2$ denoted by $\Delta^2\cong\Delta_{BCS}^2(T)(1-H/H_{c2})$. Furthermore, it depends decisively on the quantity $\Lambda/v\sin\theta$ where $\Lambda=1/\sqrt{2eH}$, v is the Fermi velocity in the plane perpendicular to $\mathbf{H}$, and θ is the angle between the quasiparticle momentum $\mathbf{p}$ and the field $\mathbf{H}$. For $\theta\to0$ the Green's functions G and F tend to the ordinary Green's functions for an s-wave superconductor with gap Δ. For finite θ, the self-

energy contains both the effects of the Doppler shift and the Andreev scattering by the potential $V(\mathbf{p}')=\Delta^2\Lambda^2\delta(p_z')\exp(-\Lambda^2 p'^2)$ for momenta $\mathbf{p}'$ in the plane perpendicular to $\mathbf{H}$. This potential is multiplied by the hole propagator $G^0(\mathbf{p}-\mathbf{p}',-\omega)$ and integrated over all $\mathbf{p}'$. The theory of α based on the Kubo formula and the BPT Green's function[13] leads in the extreme clean limit to unphysical results in the final expressions. However, for small enough mean free paths l this method is capable of describing experiments near H_{c2} sufficiently well.[17]

Another approximation scheme for α, which is based on the Eilenberger equations and the Larkin-Ovchinnikov equations for the correlation functions via linear-response theory,[14] can be carried out in the limit $l\to\infty$. In this approximation scheme only the $\mathbf{k}=0$ coefficient (spatial average) of the solution is considered. These authors state that this approximation is most questionable for quasiparticle directions $\mathbf{p}||\mathbf{H}$, and therefore they have concentrated on the special case of longitudinal ultrasonic attenuation where the wave vector $\mathbf{q}$ is parallel to $\mathbf{H}$. Then the main contributions to the correlation function arise from directions $\mathbf{p}$ perpendicular to $\mathbf{q}$, and thus perpendicular to $\mathbf{H}$, for which their approximation is best.

Since our main aim is to calculate α for unconventional superconducting gaps with nodes, we employ BPT Green's functions G and F where Δ^2 is replaced by $|\Delta f(\mathbf{p})|^2$ with $f(\mathbf{p})$ containing the $\mathbf{p}$ dependence. This result has been derived from the original spatial integral equation for $G(\mathbf{r},\mathbf{r}',\omega)$ which contains in the kernal the nonlocal order parameters $\Delta(\mathbf{r}_1,\mathbf{r}_1')$ and $\Delta^*(\mathbf{r}_2,\mathbf{r}_2')$. The method consists in writing $\Delta(\mathbf{r}_1,\mathbf{r}_1')=\Delta(\mathbf{r}_1,\mathbf{r}_1-\mathbf{r}_1')$ and $\Delta^*(\mathbf{r}_2,\mathbf{r}_2')=\Delta^*(\mathbf{r}_2,\mathbf{r}_2-\mathbf{r}_2')$ and introducing Fourier integrals with respect to the relative coordinates. In this way one can show that, to a good approximation ($p'\sim 1/\Lambda\ll p_F$), the Δ^2 in the BPT Green's function is replaced by $\Delta^2|f(\mathbf{p})|^2$.

Another problem arises from the fact that we consider α for longitidunal and transverse sound waves with propagation vector $\mathbf{q}$ in the ab plane of Sr_2RuO_4, together with a field $\mathbf{H}$ in the plane which is rotated with respect to the $\hat{\mathbf{a}}$ direction by the rotation angle Θ. This means that the angle between $\mathbf{q}$ and $\mathbf{H}$ takes on all values, including $\mathbf{q}$ perpendicular to $\mathbf{H}$ so that the main contributions to α arise from directions of $\mathbf{p}$ near the direction of $\mathbf{H}$. As has been pointed out above, for these directions the BPT Green's function is close to the ordinary Green's function which is physically quite plausible. Furthermore, for $\mathbf{p}\|\mathbf{H}$ our correlation function, Eq. (3), tends to the one derived in Ref. 18 for $H=0$. Therefore we believe that, in contrast to the semiclassical approximation scheme,[14] our method can deal quite well with general directions of $\mathbf{H}$ with respect to $\mathbf{q}$ in the ab plane.

In Sec. II we present the general theory on the basis of the BPT Green's function. In Sec. III we discuss the ultrasonic attenuation results for different sound modes and several superconducting states with vertical and horizontal line nodes. The conclusions are given in Sec. IV.

II. GENERAL THEORY OF ULTRASONIC ATTENUATION NEAR H_{c2}

Our present theory for the ultrasonic attenuation α closely follows the method for calculating the thermal conductivity in magnetic fields near H_{c2}.[12] We start with the normal and anomalous BPT Green's functions G and F which contain both the effects of supercurrent flow and scattering by the Abrikosov vortex lattice on the quasiparticle spectrum.[15] These Green's functions are employed in the expressions for the correlation functions for longitudinal and transverse sound propagation. Our method for evaluating the Kubo formula follows closely the method which has been used in the early theory of thermal conductivity by Ambegaokar and Tewordt.[19] First the integral of $\mathrm{Re}[G(\xi,\omega)\cdot G^*(\xi-\mathbf{v}\cdot\mathbf{q},\omega-\omega_0)-F\cdot F^*]$ over the energy variable ξ is carried out. Here $\mathbf{q}$ and ω_0 are the wave vector and frequency of the sound wave and $\mathbf{v}$ is the Fermi velocity. This yields the residue of this expression at the pole $\xi=\xi_0$ of the BPT Green's function $G(\xi,\omega)$ given by Eqs. (4) and (5). The most important term in the resulting expression is the quantity $\mathrm{Im}\,\xi_0$ which yields the scattering rates due to impurity scattering and Andreev scattering by the vortices [see Eq. (3)]. We have obtained the Andreev scattering rate by calculating $\mathrm{Im}\,\xi_0$ from Eqs. (4) and (5) for given ω/Δ, $\Delta\Lambda/v$, and $\gamma=0$ (no impurity scattering) as a function of the angle $\tilde{\theta}=\phi-\Theta$ between the quasiparticle direction $\mathbf{p}$ and the field $\mathbf{H}$. Then we find that for $\omega\geqslant\Delta$ (extended states) $\mathrm{Im}\,\xi_0$ is zero in a range of angles above $\tilde{\theta}=0$ ($\mathbf{p}\|\mathbf{H}$) which increases with ω, and becomes finite of order $(\Delta\Lambda/v)^2$ in a broad range of angles up to $\tilde{\theta}=\pi/2$ ($\mathbf{p}\perp\mathbf{H}$) (see Fig. 5). It should be pointed out that the denominator of the second factor in Eq. (3) (without the absolute square) occurs also in the expression for the density of states in the vortex state.[15] In the limit $\tilde{\theta}=\phi-\Theta\to 0$ ($\mathbf{p}\|\mathbf{H}$) the expression for I in Eq. (3) (for $ql\to 0$) tends to the well-known expression for the inverse relaxation rate $\mathrm{Im}\,\xi_0\to\mathrm{Im}(\tilde{\omega}^2-|\Delta|^2)^{1/2}$ (where $\tilde{\omega}=\omega+\imath\gamma$) times the coherence factor $1+(|\tilde{\omega}|^2-|\Delta|^2)/|\tilde{\omega}^2-|\Delta|^2|$ which was first derived in Appendix C of Ref. 19. In the hydrodynamic regime, $\omega_0\tau\ll 1$, we obtain, by including vertex corrections in analogy to Ref. 18, the following expression for the ratio of the ultrasound attenuation in the superconducting state α_s to that in the normal state α_n:

$$\frac{\alpha_s}{\alpha_n}=\int_0^\infty\frac{d\omega}{2T}\,\mathrm{sech}^2(\omega/2T)\left\{\int_0^{2\pi}\frac{d\phi}{2\pi}[\pi_{ij}(\phi)]^2 I(\phi)+\left[\int_0^{2\pi}\frac{d\phi}{2\pi}[\pi_{ij}(\phi)]I(\phi)\right]^2\left[|g|^2-\int_0^{2\pi}\frac{d\phi}{2\pi}I(\phi)\right]^{-1}\right\},\tag{1}$$

where

$$\pi_{xx}^2(\phi)=2\cos^2(2\phi),\quad (L100);$$

$$\pi_{xy}^2(\phi)=2\sin^2(2\phi),\quad (T100),\tag{2}$$

$$I(\phi)=\frac{\mathrm{Im}\,\xi_0/\Gamma}{[(\mathrm{Im}\,\xi_0/\Gamma)^2+(ql)^2(\hat{q}\cdot\hat{p})^2]}\times\frac{\{1-\pi[\Delta\Lambda/v\,\sin(\phi-\Theta)]^2|f|^2|w(z_0)|^2\}}{|1+2[\Delta\Lambda/v\,\sin(\phi-\Theta)]^2|f|^2[1+i\sqrt{\pi}z_0w(z_0)]|^2},\tag{3}$$

$$z_0=(\omega+i\gamma+\xi_0)[\Lambda/v\,\sin(\phi-\Theta)],\quad \Lambda=(2eH)^{-1/2},$$

$$\gamma=\Gamma/g,\quad g=N(\omega,H)/N_0.\tag{4}$$

Here π_{xx}^2 and π_{xy}^2 are the weight factors for the $L100$ ($T110$) and $T100$ ($L110$) sound modes[7,10] where L = longitudinal, T = transverse, and $\hat{\mathbf{q}}\|[100]$ or $[110]$. We use the following notation: Γ is the normal-state impurity scattering rate, v is the in-plane Fermi velocity, $\Theta=\angle(\mathbf{H},\hat{\mathbf{a}})$ is the direction of $\mathbf{H}$ in the ab plane, Δ^2 is the spatial average of the absolute square of the order parameter for the Abrikosov vortex lattice, and $|f(\phi)|^2$ is the normalized absolute square of the gap function. The quantity z_0, and thus the pole ξ_0 of G, is given by the transcendental equation[15,12]

$$z_0=2(\omega+i\gamma)[\Lambda/v\,\sin(\phi-\Theta)]+i\sqrt{\pi}[\Delta\Lambda/v\,\sin(\phi-\Theta)]^2|f|^2w(z_0).\tag{5}$$

Here, $w(z)=\exp(-z^2)erfc(-\imath z)$. Note that Eqs. (4) and (5) differ from the corresponding equations in Ref. 15 in that the $\sin\theta$ in the original quantity $\Delta\Lambda/v\,\sin\theta$ is replaced by $\sin(\phi-\Theta)$ for $\mathbf{p}$ lying in the direction ϕ and $\mathbf{H}$ lying in the direction Θ in the ab plane, and Δ^2 is replaced by $\Delta^2|f(\phi)|^2$ for a gap with vertical lines of nodes. For a general state with $f(\mathbf{p})$ one has to replace $\sin\theta$ with the expression given in Eq. (7) of Ref. 12 and carry out the double integral over the polar and azimuthal angles θ and ϕ. In the following calculations we will neglect the term proportional to $(ql)^2$ in the first denominator of Eq. (3) assuming the long-wavelength limit $ql\ll 1$. The dependencies of $(\Delta\Lambda/v)^2$ and $(\Lambda/v)^2$ on H/H_{c2} are presented in Ref. 12. The expression for ultrasonic attenuation in Eq. (1) is similar to the expression for κ in Ref. 12 apart from the missing factor ω^2, the weight factor π_{ij}^2 instead of v_i^2, and the vertex corrections [second term in the curly brackets in Eq. (1)]. For the vertex corrections we have used the expressions in Ref. 18 for the unitary limit $\delta_N=\pi/2$ of the phase shift for impurity scattering. In the limit $\omega\to 0$, an analytical expression for the solution $z_0=ix_0$ of Eq. (5) is obtained which yields, in close analogy to κ,[12] a much simpler expression for α_s/α_n in the limit $T\to 0$.

III. RESULTS AND DISCUSSION OF ULTRASONIC ATTENUATION FOR DIFFERENT SOUND MODES AND SEVERAL SUPERCONDUCTING STATES WITH VERTICAL AND HORIZONTAL LINE NODES

First we consider the f-wave pairing state $\mathbf{d}=\Delta\hat{\mathbf{z}}(p_x+ip_y)(p_x^2-p_y^2)$ for which $|f|^2=\cos^2(2\phi)$ has four vertical line nodes at $\phi=\pi/4,3\pi/4,\ldots$ on the cylindrical Fermi surface. In Fig. 1 we show our results for α_s/α_n versus H/H_{c2} for the $L100$ ($\Theta=0$) and $T100$ ($\Theta=\pi/4$) modes at $T=0$ and impurity scattering rate $\Gamma/\Delta_0=0.1$. Δ_0 is the BCS gap parameter, and we will always use the value $\beta_A=1.2$ for the Abrikosov parameter. It is seen that α_s/α_n for the $L100$ mode exhibits a strong upward curvature near H_{c2} while it is a more linear function of H for the $T100$ mode. For increasing Γ/Δ_0 the upward curvatures decrease.

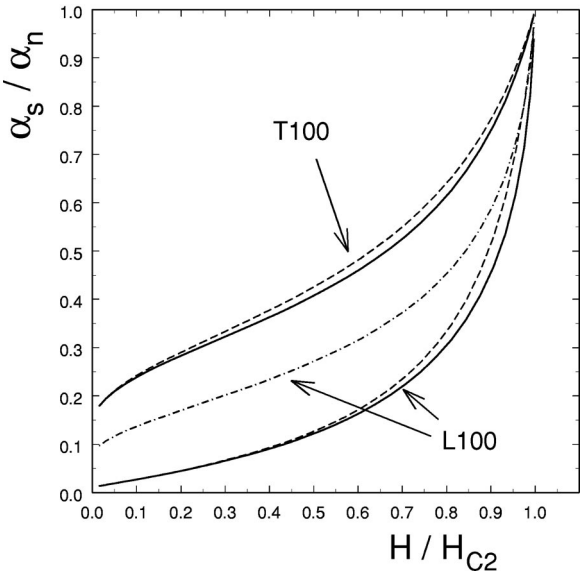

FIG. 1. Ultrasonic attenuation α_s/α_n vs applied field H/H_{c2} at $T=0$ for longitudinal and transverse in-plane sound modes $L100$ ($\Theta=0$; $\Theta=\angle(\mathbf{H},\hat{\mathbf{a}})$) and $T100$ ($\Theta=\pi/4$) for impurity scattering rate $\Gamma/\Delta_0=0.1$. Vertical gap nodes: solid and dashed curves without and with vertex corrections in the unitary impurity scattering limit, respectively. Horizontal gap nodes: dash-dot curve.

The solid curves for α_s/α_n in Fig. 1 are calculated by neglecting the vertex corrections in Eq. (1), while the dashed curves include the vertex corrections in the unitary impurity scattering limit. One recognizes that the effect of the vertex corrections in the unitary limit is rather small. This is also true for impurity scattering in the Born limit where $|g|^2$ in the denominator of Eq. (1) is replaced by 1. It is interesting that, for field direction angles $\Theta=\pi/4$ and $\Theta=0$, the vertex corrections for the $L100$ and $T100$ modes, respectively, vanish. In the following calculations and figures we shall neglect the vertex corrections.

In Fig. 2 we show the dependence of α_s/α_n on the in-plane field direction Θ at $T=0$ for fixed field strength, $\Delta\Lambda/v=0.2$, and impurity scattering rate $\Gamma/\Delta_0=0.1$. One sees that $\alpha(\Theta)$ has variations in Θ of fourfold symmetry where the minima and maxima occur at $\Theta=0$ and $\pi/4$ for the $L100$ mode. For the $T100$ mode the maxima and minima are reversed. The maxima and minima can be explained as an effect of the ϕ dependence of the weighting factors π_{ij}^2 in Eq. (2) and the density of states since the expression $|\cdots|^{-2}$ in the denominator of $I(\phi)$ in Eq. (3) is proportional to $|N(\phi,\Theta)|^2$. The density of states has a minimum (maximum) for quasiparticles traveling parallel (perpendicular) to the field.[15] The minima for $L100$ and $T100$ occur at $\Theta=0$ and $\pi/4$, respectively, because the corresponding weight fac-

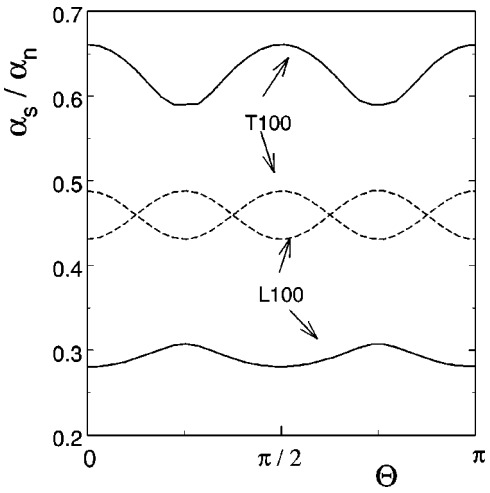

FIG. 2. α_s/α_n vs $\Theta=\angle(\mathbf{H},\hat{\mathbf{a}})$ for in-plane field rotation at $T=0$ for sound modes $L100$ and $T100$ and gap parameter $\Delta\Lambda/v=0.2(H/H_{c2}=0.78)$ and $\Gamma/\Delta_0=0.1$. Solid curves: vertical gap nodes. Dashes curves: horizontal gap nodes.

tors π_{xx}^2 and π_{xy}^2 have maxima at $\Theta=0$ and $\pi/4$. For higher fields (e.g., $\Delta\Lambda/v=0.1$) a small local maximum and two neighboring minima occur around $\Theta=\pi/4$ for the $T100$ mode due to the node of the gap at $\Theta=\pi/4$.

The sound attenuation for the other *f*-wave pairing state, proportional to $p_x p_y$ with $|f|^2=\sin^2(2\phi)$, is obtained from the previous expression for $|f|^2=\cos^2(2\phi)$ by a simple transformation, $\phi'=\phi-\pi/4$, in Eq. (1). This exchanges the results for $L100$ and $T100$ which become functions of the new field rotation angle $\Theta'=\Theta-\pi/4$.

We consider now the spin-triplet pairing state with horizontal line nodes[9] where the squared gap amplitude is proportional to $|f|^2=\cos^2(cp_z)=\cos^2[\chi]$. Then, in addition to the ϕ integration in Eq. (1), one also has to do the integration over χ from $-\pi$ to $+\pi$. In Fig. 1 we have included our result for α_s/α_n versus H/H_{c2} for the mode $L100$ at $T=0$ and $\Gamma/\Delta_0=0.1$. A strong upward curvature occurs near H_{c2} which is similar to that of the $L100$ mode for vertical nodes, but is quite distinct from the almost linear dependence of α_s/α_n on H/H_{c2} for the $T100$ mode in the case of vertical nodes. In Fig. 2 we have plotted our results for the in-plane field variation $\alpha(\Theta)$ for the $L100$ and $T100$ modes. Note that the function $\alpha(\Theta)$ for $T100$ is obtained by shifting the function for $L100$ by $\Theta=\pi/4$ along the Θ axis. This can be seen by a variable transformation $\phi'=\phi-\pi/4$ in Eqs. (1)–(3) making use of the fact that $|f|^2=\cos^2(\chi)$ does not depend on ϕ. Comparison of the curves in Fig. 2 shows that the amplitudes of the variations $\alpha(\Theta)$ for vertical and horizontal nodes are about the same (here about 10%). However, there is a marked difference in the form of the variations for the $L100$ and $T100$ modes for vertical nodes because, for the $T100$ mode, the gap node manifests itself in the structure around $\pi/4$. In contrast to this, the form of the variations for horizontal nodes is the same apart from the shift by $\pi/4$ along the Θ axis.

We turn now to the ω dependence of the ϕ integrals in Eq. (1) which determine the T dependence of α_s/α_n. It is

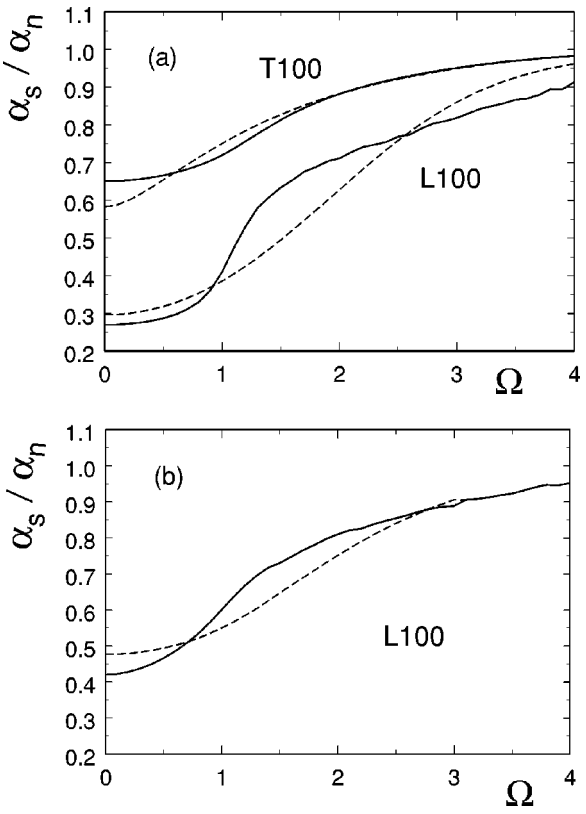

FIG. 3. Integrand $\alpha_s(\Omega)/\alpha_n$ in Eq. (1) for α_s/α_n [without the factor $(1/2T)\mathrm{sech}^2(\omega/2T)$] vs reduced frequency $\Omega=\omega/\Delta$ for gap parameter $\Delta\Lambda/v=0.2(H/H_{c2}=0.78)$ and field directions $\Theta=0$ (solid curves) and $\Theta=\pi/4$ (dashed curves), and $\Gamma/\Delta_0=0.1$. (a) $L100$ and $T100$ for vertical gap nodes; (b) $L100$ for horizontal gap nodes.

now necessary to solve Eq. (5) for z_0 as a function of $\Omega=\omega/\Delta$, and then to integrate the resulting expression for $I(\phi)$ in Eq. (3) [multiplied by $\pi_{ij}^2(\phi)$, etc.] over ϕ (and χ for horizontal nodes). We denote by $\alpha_s(\Omega)/\alpha_n$ the resulting integrand of the ω integral [without the factor $(1/2T)\mathrm{sech}^2(\omega/2T)$]. In Fig. 3(a) we plot $\alpha_s(\Omega)/\alpha_n$ vs Ω for $|f|^2=\cos^2(2\phi)$ for large field magnitude $[\Delta\Lambda/v=0.2(H/H_{c2}=0.78)]$ and field directions $\Theta=0$ and $\pi/4$ for both the $L100$ and $T100$ modes. It is interesting that the curves for $\Theta=0$ and $\pi/4$ cross at finite frequencies Ω which means that the minima and maxima in $\alpha(\Theta)$ are interchanged. Furthermore, the Ω dependence for $T100$ at $\Theta=\pi/4$ is almost linear while, for $L100$ and $\Theta=0$, it is quadratic. In Fig. 3(b) we show $\alpha_s(\Omega)/\alpha_n$ for the state $|f|^2=\cos^2(cp_z)$.

The temperature dependence of α_s/α_n is obtained according to Eq. (1) by integrating the expression $(1/2T)\mathrm{sech}^2(\omega/2T)\alpha_s(\Omega)/\alpha_n$ over ω. For the variable transformation from ω to $\Omega=\omega/\Delta$ we make use of the relations $\Delta/\Delta_0=[1-(H/H_{c2})]^{1/2}/\sqrt{\beta_A}$ and $H/H_{c2}=[1+6\beta_A(\Delta\Lambda/v)^2]^{-1}$.[12] In Fig. 4 we show our results for α_s/α_n vs T/T_c for vertical gap nodes at low- and high-field strength ($\Delta\Lambda/v=0.6$ and 0.2, or $H/H_{c2}=0.28$ and 0.78) and field directions $\Theta=0$ and $\Theta=\pi/4$ for the $L100$ and $T100$ modes. One recognizes that, for low T, the attenuation of the

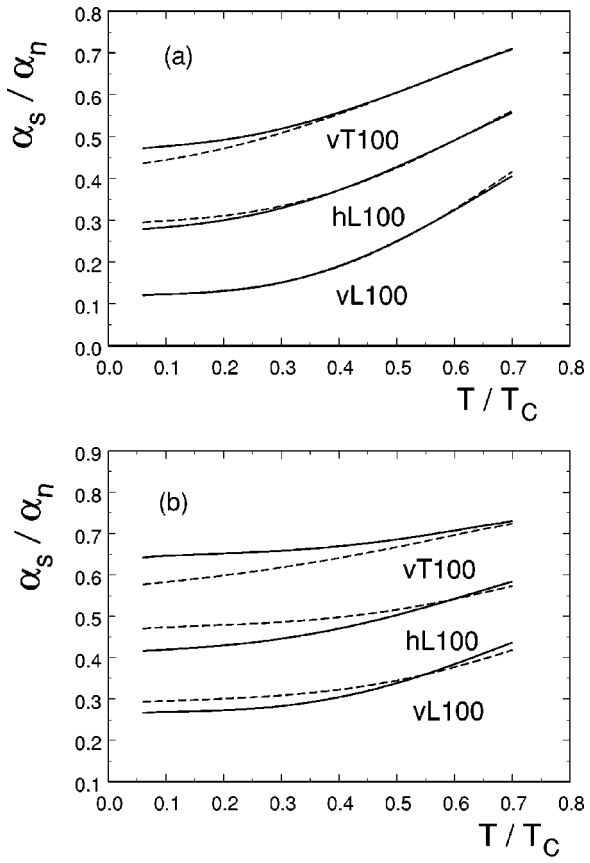

FIG. 4. α_s/α_n vs T/T_c for $vL100$, $vT100$, and $hL100$ (v = vertical, h = horizontal gap nodes), for field directions $\Theta=0$ (solid curves) and $\Theta=\pi/4$ (dashed curves). (a) $\Delta\Lambda/v=0.6(H/H_{c2}=0.28)$, $\Gamma/\Delta_0=0.2$; (b) $\Delta\Lambda/v=0.2(H/H_{c2}=0.78)$, $\Gamma/\Delta_0=0.1$.

$L100$ mode is approximately a quadratic function of T, while it is nearly linear for the $T100$ mode at $\Theta=\pi/4$. These different low T power laws for the $L100$ and $T100$ modes agree roughly with the results of Ref. 10 for zero field. It is interesting that the quadratic and linear T dependencies of α_s/α_n for the $L100$ and $T100$ modes correspond to the quadratic and linear dependencies of α_s/α_n on H/H_{c2} for these modes (see Fig. 1). In Fig. 4 we also show α_s/α_n vs T/T_c for the $L100$ mode for horizontal gap nodes and field directions $\Theta=0$ and $\pi/4$. We recall that the results for $L100$ for $\Theta=0(\pi/4)$ are identical to those for $T100$ for $\Theta=\pi/4(0)$. One sees that the dependence on T is nearly quadratic.

IV. CONCLUSIONS

In summary, we have calculated the ultrasonic attenuation α in layered Sr_2RuO_4 in the presence of in-plane magnetic fields for spin-triplet superconducting states with vertical or horizontal line nodes in the gap. This theory takes into account the effects of supercurrent flow and Andreev scattering (see Fig. 5) by the Abrikosov vortex lattice near H_{c2}. For rotating in-plane field $H(\Theta)$ the attenuation $\alpha(\Theta)$ exhibits variations of fourfold symmetry in the rotation angle Θ. At $T=0$ the minima occur at $\Theta=0$ and $\pi/2$ for the $L100$ sound mode, and at $\Theta=\pi/4$ and $3\pi/4$ for the $T100$ mode. The

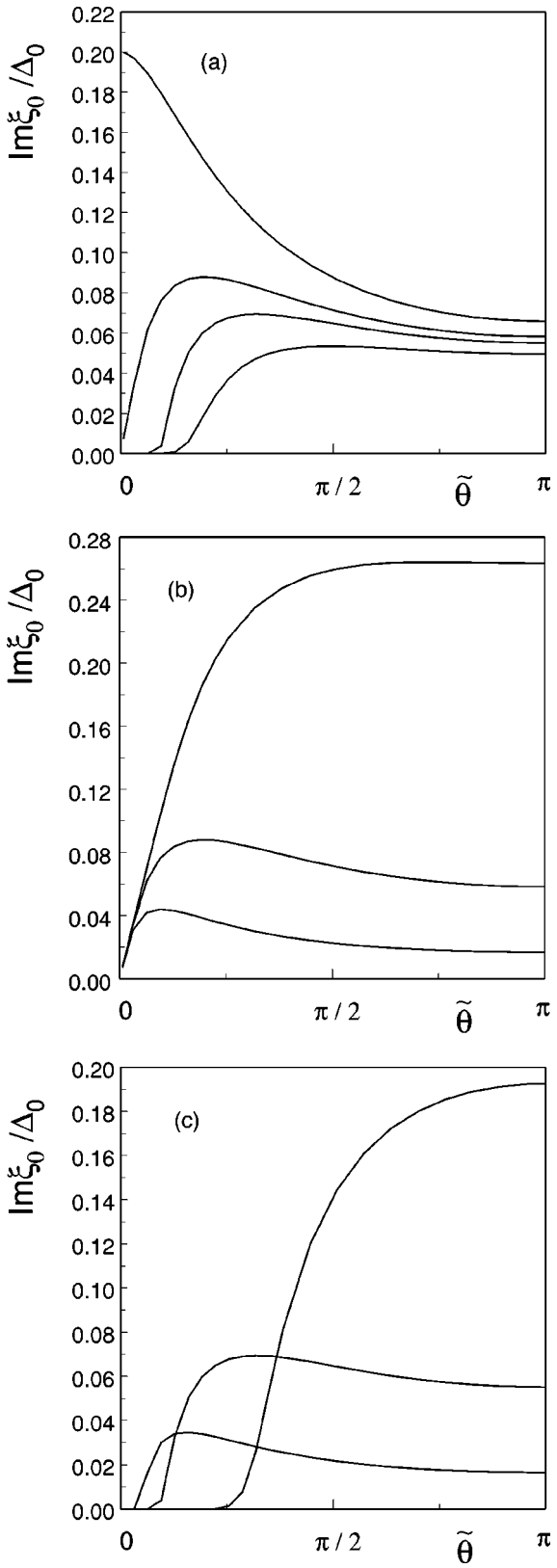

FIG. 5. Andreev scattering given by $\mathrm{Im}\,\xi_0/\Delta_0$ (for $\gamma=0$), versus $\tilde{\theta}=\angle(\mathbf{p},\mathbf{H})$ for fixed $\tilde{\Delta}=\Delta\Lambda/v\approx[(H_{c2}/H)-1]^{1/2}/\sqrt{6\beta_A}$ and $\Omega=\omega/\Delta$. (a) $\tilde{\Delta}=0.2$ and $\Omega=0.0$, 1.0, 1.2, and 1.5 (from top to bottom); (b) $\Omega=1.0$ and $\tilde{\Delta}=0.6$, 0.2, and 0.1 (from top to bottom); (c) $\Omega=1.2$ and $\tilde{\Delta}=0.6$, 0.2, and 0.1 (from top to bottom).

amplitudes of the variations are about the same ($\approx 10\%$) for both horizontal and vertical nodes. However, in the case of vertical nodes, $\alpha(\Theta)$ for the $T100$ mode shows characteristic structure in the directions of the nodes. For horizontal nodes the variations $\alpha(\Theta)$ for the $L100$ and $T100$ modes are the same if Θ is shifted by $\pi/4$. The distinction between vertical and horizontal nodes also manifests itself in the different field and temperature dependencies of α. For vertical nodes the ratio α_s/α_n exhibits a strong upward curvature as a function of H/H_{c2} near H_{c2} for the $L100$ mode while it is more linear for the $T100$ mode. In the case of horizontal nodes, the attenuation for both the $L100$ and $T100$ modes shows a strong upward curvature near H_{c2}. The temperature dependence of the sound attenuation is determined by the frequency dependence of the integrand $\alpha(\Omega)$, $\Omega=\omega/\Delta$, in the expression for α_s/α_n. It is interesting that the curves for the functions $\alpha(\Omega)$ for field directions $\Theta=0$ and $\pi/4$ cross each other twice for increasing Ω indicating that the maxima and minima are interchanged twice. This causes corresponding crossings in the T dependencies of α for the two field directions. For vertical gap nodes, at low T, α_s/α_n exhibits approximately a T^2 power law for the $L100$ mode and a roughly linear T dependence for the $T100$ mode. For horizontal gap nodes the functions α_s/α_n vs T/T_c for the $L100$ and $T100$ modes are identical for field direction differing by $\pi/4$. For low and high fields α_s/α_n follows roughly a T^2 power law.

The ultrasonic attenuation in Sr_2RuO_4 in zero field has been measured for the four in-plane modes $L100$, $T110$, $T500$, and $L110$.[7] The attenuation follows a low-temperature power law $T^{1.8}$ for the $L100$ ($T110$) mode and $T^{1.4}$ for the $T100$ mode. In Ref. 8 a T^2 power law below T_{imp} and a T^3 dependence above T_{imp} has been measured for the $T110$ mode. Calculations based on the assumption of a circular cylindrical Fermi surface and vertical gap nodes[10] yield a linear T dependence of α_s/α_n for the $T100$ ($L110$) mode which disagrees with the measured $T^{1.4}$ power law and, for the $L100$ mode, a power law close to the measured one. The fact that the weakest T dependence occurs for the $T100$ mode is taken as an indication[7] that the gap nodes point in the [110] direction because this yields an excess of quasiparticles with wave vectors in this direction.

Our results for the ultrasound attenuation for vertical nodes in magnetic fields up to H_{c2} also yield the weakest (linear) H and T dependence for the $T100$ mode because the corresponding weight factor has a maximum in the direction of a vertical gap node. Our calculations yield a stronger (quadratic) H and T dependence for the $L100$ mode because the corresponding weight factor has a maximum in the direction of a vertical gap antinode. This is in strong contrast to the case of horizontal line nodes where we obtain a roughly quadratic H and T dependence for *both* the $L100$ and $T100$ modes, which are actually identical for in-plane field directions differing by $\pi/4$.

At this point we would like to mention the modifications required if one takes the model of horizontal line nodes suggested in Ref. 7. This model can be simulated by multiplying the $\cos(cp_z)$ used in this paper (see Ref. 9) by a gap with

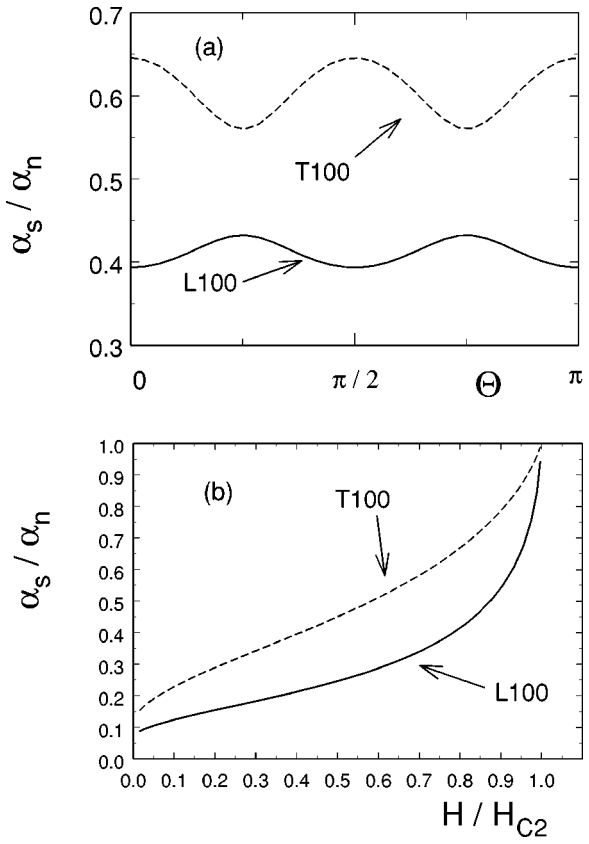

FIG. 6. α_s/α_n for a gap with horizontal line nodes and fourfold angular modulation in the plane ($\lambda=1/2$) for the $L100$ (solid curves) and $T100$ (dashed curves) sound modes. (a) α_s/α_n vs $\Theta=\angle(\mathbf{H},\hat{\mathbf{a}})$ for $H/H_{c2}=0.78$; (b) α_s/α_n vs H/H_{c2} at $T=0$ and for $\Gamma/\Delta_0=0.1$.

fourfold angular modulation, $(1+\lambda\cos 4\phi)$, $0<|\lambda|<1$, in the plane. This has the effect that the dashed curves in Fig. 2 for the variations $\alpha(\Theta)$ of the $L100$ and $T100$ modes drift apart with a shift (and thus the anisotropy) that increases with increasing amplitude λ of the fourfold gap modulation. See Fig. 6(a) for the case $\lambda=1/2$. Corresponding splittings occur in the attenuation curves α versus the field (Fig. 1) and temperature (Fig. 4) for the $L100$ ($T110$) and $T100$ modes which are identical in our simple model of horizontal line nodes [see Fig. 6(b)]. In fact, the H and T dependencies of α for the $T100$ mode become weaker than those of the $L100$ mode for increasing amplitude λ of the gap modulation. We remark that such a fourfold angular modulation occurs in the gaps of the passive α and β bands where horizontal line nodes are induced by the nodeless p-wave gap in the active band by interband proximity effect.[20] We have fitted this gap modulation in the passive bands with our gap model discussed above and estimate a rather small value for λ of about 0.1. The p-wave gap without line nodes is approximated in this model with $\lambda=-0.69$.[21] For this p-wave gap the attenuation curves for the $T100$ and $L100$ modes in Figs. 1 and 2 (solid curves) are, roughly speaking, interchanged, which is plausible because the gap minima occur in the directions $\phi=0,\pi/2,\ldots$. This has the effect that the H and T dependen-

cies of α for the $L100$ mode become weaker than those of the $T100$ mode. This appears to be in disagreement with experiment.[7]

It should be pointed out that our theory is based on a number of simplifying assumptions. First, we have considered only the lowest-order Fourier coefficient of the Green's functions with respect to the reciprocal Abrikosov vortex lattice. As the field decreases, the higher Fourier coefficients become more and more important and, near H_{c1}, the Doppler-shift method for a single vortex becomes more appropriate. Second, we have assumed a cylindrical single sheet Fermi surface, whereas the huge anisotropy observed between the $T110$ and $T100$ normal-state attenuation coefficients[7] indicates that the anisotropy follows from the nature of the three orbitals forming the three sheets of the Fermi surface in Sr_2RuO_4.[22] These authors showed that in the case of Sr_2RuO_4 a simple viscosity tensor describing the electron-phonon interaction may not be sufficient for ultrasound attenuation. If this is the case our predictions could be changed. Third, we have assumed that the attenuation coefficients normalized to their normal-state values are insensitive to the observed normal-state anisotropies. Here we have taken a temperature-independent scattering rate Γ giving rise to a temperature-independent normal-state attenuation which agrees roughly with the data for the $L100$ and $T100$ modes.[7] Thus it cannot be excluded that the effect of the normal-state anisotropy exceeds all anisotropies in the superconducting state calculated in this work.

In spite of the above uncertainties we believe that measurements of the field dependencies (in addition to the temperature dependencies) of the ultrasonic attenuation for different in-plane sound modes can still provide useful information about the nodal structure of the energy gap in Sr_2RuO_4.

ACKNOWLEDGMENTS

We thank K. Scharnberg, N. Schopohl, and T. Dahm for helpful discussions.

[1] Y. Maeno, H. Hasimoto, K. Yoshida, S. Nishizaki, T. Fujita, J. G. Bednorz, and F. Lichtenberg, Nature (London) **372**, 532 (1994).
[2] S. NishiZaki, Y. Maeno, and Z. Mao, J. Low Temp. Phys. **117**, 1581 (1999); J. Phys. Soc. Jpn. **69**, 572 (2000).
[3] K. Ishida, H. Mukuda, Y. Kitaoka, Z. Q. Mao, Y. Mori, and Y. Maeno, Phys. Rev. Lett. **84**, 5387 (2000).
[4] K. Izawa, H. Takahashi, H. Yamaguchi, Yugi Matsuda, M. Suzuki, T. Sasaki, T. Fukase, Y. Yoshida, R. Settai, and Y. Onuki, Phys. Rev. Lett. **86**, 2653 (2001).
[5] M. A. Tanatar, M. Suzuki, S. Nagai, Z. Q. Mao, Y. Maeno, and T. Ishiguro, Phys. Rev. Lett. **86**, 2649 (2001).
[6] I. Bonalde, B. D. Yanoff, M. B. Salamon, D. J. Van Harlingen, E. M. E. Chia, Z. Q. Mao, and Y. Maeno, Phys. Rev. Lett. **85**, 4775 (2000).
[7] C. Lupien, W. A. MacFarlane, C. Proust, L. Taillefer, Z. Q. Mao, and Y. Maeno, Phys. Rev. Lett. **86**, 5986 (2001).
[8] H. Matsui, Y. Yoshida, A. Mukai, R. Settai, Y. Onuki, H. Takei, N. Kimura, H. Aoki, and N. Toyota, Phys. Rev. B **63**, 060505(R) (2001).
[9] Y. Hasegawa, K. Machida, and M. Ozaki, J. Phys. Soc. Jpn. **69**, 336 (2000).
[10] M. J. Graf and A. V. Balatsky, Phys. Rev. B **62**, 9697 (2001).
[11] T. Dahm, H. Won, and K. Maki, cond-mat/0006301 (unpublished).
[12] L. Tewordt and D. Fay, Phys. Rev. B **64**, 24 528 (2001).
[13] K. Scharnberg, J. Low Temp. Phys. **6**, 51 (1972).
[14] P. Klimesch and W. Pesch, J. Low Temp. Phys. **32**, 869 (1978).
[15] U. Brandt, W. Pesch, and L. Tewordt, Z. Phys. **201**, 209 (1967).
[16] W. Pesch, Phys. Lett. **28B**, 71 (1968); Ph.D. thesis, Hamburg, 1968.
[17] A. Houghton and K. Maki, Phys. Rev. B **4**, 843 (1971).
[18] K. Scharnberg, D. Walker, H. Monien, L. Tewordt, and R. A. Klemm, Solid State Commun. **60**, 535 (1986).
[19] V. Ambegaokar and L. Tewordt, Phys. Rev. **134**, A805 (1964).
[20] M. E. Zhitomirsky and T. M. Rice, Phys. Rev. Lett. **87**, 057 001 (2001).
[21] K. Miyake and O. Narikiyo, Phys. Rev. Lett. **83**, 1423 (1999).
[22] M. B. Walker, M. F. Smith, and K. V. Samokhin, cond-mat/0105109 (unpublished).